Radio Frequency Microdischarge Neutraliser

IEPC-2019-214

Presented at the 36th International Electric Propulsion Conference
University of Vienna, Austria
September 15-20, 2019

Félicien Filleul *
Te Pūnaha Ātea - Auckland Space Institute, The University of Auckland, Auckland, 1010, New Zealand

Christine Charles † and Rod Boswell‡
Space Plasma, Power and Propulsion Laboratory, Australian National University, Canberra, 2601, Australia

Nicholas Rattenbury§ and John Cater¶
Te Pūnaha Ātea - Auckland Space Institute, The University of Auckland, Auckland, 1010, New Zealand

Orson Sutherland‖
European Space Agency - ESTEC, Noordwijk, 2201AZ, The Netherlands

Abstract: A new plasma propulsion experimental apparatus has been set up at the University of Auckland in collaboration with the Australian National University. The first research focuses on exploring the potential of a novel millimetric scale capacitively coupled, low power radio frequency plasma device as an alternative to hollow cathodes for primary plasma and electron source in conventional ion thruster technologies. The electron Pocket Rocket neutraliser, ePR, has inherent advantages over hollow cathodes: the driven electrode is not in contact with the plasma, which enables longer operational lifetime and the device can produce a high density plasma (~$10^{18}\,\mathrm{m}^{-3}$) instantly (~μs) compared to the several minutes required for hollow cathodes. In a preliminary study, two modes of operation have been identified for routine operational conditions ranging $\in [2, 24]$ W and $\in [0.7, 2.0]$ Torr. A high current mode gives electron currents in excess of 25 mA. There, current scales with input power, argon pressure and negative bias on an internal electrode which collects an equal amount of ion current. A low current mode has electron currents $\in [1, 3.5]$ mA and occurs when the internal electrode is grounded. In this mode, current scales with input power and decreasing operational argon pressure. An electron current of 41 mA was achieved at 2.0 Torr and ~50 W with the ion electrode biased at -320 V.

*PhD student, Department of Physics, ffli056@aucklanduni.ac.nz.
†Professor and Head, Centre for Plasmas and Fluids, Research School of Physics, christine.charles@anu.edu.au.
‡Professor, Centre for Plasmas and Fluids, Research School of Physics, Rod.Boswell@anu.edu.au.
§Senior Lecturer, Department of Physics, n.rattenbury@auckland.ac.nz.
¶Senior Lecturer, Department of Engineering Science, j.cater@auckland.ac.nz.
‖Spacecraft Development Manager, Directorate of Human Spaceflight and Robotic Exploration , Orson.Sutherland@esa.int.

Nomenclature

ePR	= electron Pocket Rocket neutraliser	e	= Elementary charge
RF	= Radio Frequency	u_B	= Bohm velocity
LPP	= Langmuir Probe - Plenum	λ_D	= Debye length
LPC	= Langmuir Probe - Chamber	Φ_p	= Plasma potential
PE	= Plenum Electrode	Φ_f	= Plasma floating potential
CE	= Chamber Electrode	T_e	= Electron temperature
ER	= Exit Ring	T_i	= Ion temperature
P_{rf}	= RF input power	m_e	= Electron mass
P_s	= Plenum Pressure	M	= Ion mass

I. Introduction

Hollow cathodes have been the preferred electron sources for primary plasma discharge as well as for providing current and space-charge neutralisation for ion thruster technologies.[1] While capable of reliably delivering high current densities (1 to $10\,\mathrm{A \cdot cm^2}$) to satisfy most space mission requirements,[2,3] wear and fatigue of some critical components[4,5] as well as a dependency on operational environmental conditions[6] mean that hollow cathodes limit the lifetime of ion gridded and Hall effect thrusters as well as being a critical single point of failure. Depletion of the electron emitting insert, erosion of the keeper electrode and cathode tip from ion sputtering as well as failure of the heater are examples of such weaknesses.
Hollow cathodes have theoretical and experimentally validated lifetimes of over a few tens of thousands of hours[1,7] in excess of most electric propulsion (EP) mission requirements.[8,9] However, as the number of EP missions is foreseen to significantly increase in the near future,[10] missions with more ambitious goals requiring extended equivalent lifetimes at higher powers motivate us to explore electrodeless plasma sources as replacements to hollow cathodes.[11] Alternatively, the scaling down of ion thrusters for the CubeSat platform requires low power, small scale and inexpensive electron sources for ion beam neutralisation whereas a hollow cathode requires at least a few tens of Watts to operate, especially for powering the heater element.[1,12] Radio Frequency (RF) plasma sources avoid some of these limitations as they do not require doped materials as a source of electrons, nor a heater to trigger the thermionic electron emission, nor a keeper electrode.[13] Their potential is now recognized in the domain of CubeSat electric propulsion.[14]

The use of an asymmetrical capacitively coupled RF plasma discharge, derived from the Tiny Pocket Rocket (PR) electrothermal micro-thruster,[15,16] is proposed as an alternative low power electron source. In development at the Australian National University (ANU), the Pocket Rocket works on neutral gas heating by volumetric interactions with the RF plasma discharge ions at 13.56 MHz. It is able to deliver thrust in the order of $1-2\,\mathrm{mN}$ with ~10 W of input power.[15,17] ePR, an electron source derived from the PR system, presents several advantages over conventional hollow cathodes. ePR driven electrode is shielded from the plasma by a ceramic insert and is therefore not subject to erosion. As the discharge does not rely on thermionic electron emission, there is no concern about depletion or contamination of the electrode. In turn, the self-bias charging of the plasma discharge ceramic cavity is critical to the higher density gamma mode which promises high electron current densities at the exit of the cavity.[15,18] Operating in choked flow mode, the PR plasma discharge is also decoupled from downstream environmental conditions and the plasma generation processes are uncorrelated with the thruster ion beam plasma parameters. The transition from spot mode to an undesirable plume mode, which is typical in hollow cathodes, is therefore unexpected. As no heater element is required, ePR is an "instant-on" device. Equilibrium operation occurs over a timescale of microseconds,[17] in contrast to several minutes for hollow cathodes.[1] This could enable conventional ion thrusters to have much faster switch on times, of interest for orbit manoeuvres with short sunlight phases. Finally, ePR could also be used as a stand-alone subsystem on missions such as space tethers or as a spacecraft charging mitigation device, when fitted with its own DC-RF inverter power supply and gas storage and delivery system.[16]

This paper is arranged as follows. Firstly, the experimental plasma apparatus is presented together with the workings of the Pocket Rocket. The design modifications of a prototype acquired from ANU and attempts to enhance the electron extraction are explained. Next, the first experimental results are reported. Plasma parameters upstream and downstream of the discharge cavity, at the locations where ions and electrons are extracted respectively, were measured with single tip uncompensated Langmuir probes. There, the plasma densities are found to be $\sim 1-2 \cdot 10^{17}\,\mathrm{m}^{-3}$ for 15 W of RF power. Electron currents ranging between $[1, 25]$ mA are extracted with a disk Chamber Electrode (CE) positively biased at 30 V located in the plasma plume. The electron current is a function of the input RF power, of the ePR operational argon pressure in the discharge tube and of the bias applied to the Plenum Electrode (PE): a hollow cylindrical electrode collecting an equivalent ion current in the plenum for current balance.

II. Plasma and Electron Source

A. The Pocket Rocket

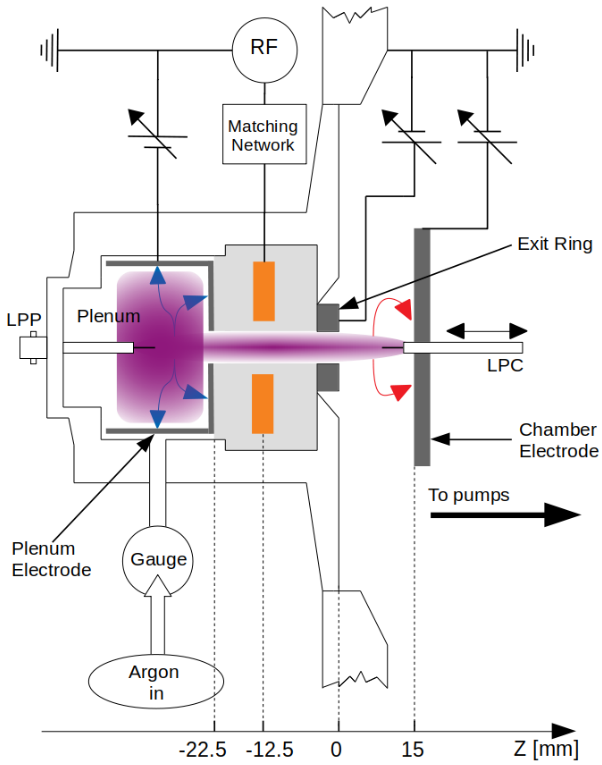

Figure 1. Sketch of the ePR electron source. In dark gray, the collecting and biasing electrodes, from left to right: the plenum ion electrode (PE), the exit ring (ER) and the chamber electron collection electrode (CE). The RF driving electrode (orange) is encapsulated into a machinable ceramic block (light gray) and connected to a 50 W RF power supply through an impedance matching network. A fixed position Langmuir probe is used in the plenum while an axially movable one is used to probe the downstream plasma properties. The blue arrows represent the ion current while the red ones the electron current.

Developed at the Australian National University (ANU), the Pocket Rocket family belongs to the class of electrothermal thrusters.[19] In such devices, thrust is produced mainly by collisional and conductive heating of a directional neutral gas flow, instead of from the acceleration of heavy ions. Therefore, Pocket Rocket can be operated in both neutral "cold" mode and plasma "hot" mode. The plasma mode is characterized by an increase of both thrust and I_{sp} compared to the cold gas operation.

Neutral gas (typically argon, nitrogen or xenon) is injected into a plenum cavity through a regulated gas inlet (left of Fig. 1). The other end of the device is connected to a vacuum chamber or exposed to space (right of Fig. 1). The two extremities are connected by a 4.2 mm diameter, 16.5 mm long ceramic tube forming the plasma cavity. A pressure gradient establishes itself along the tube, varying between 2:1 to 4:1 depending on the set mass-flow rate and pumping speed. It has been demonstrated that for a pressure gradient above $\sim$2, the flow becomes choked as the gas reaches sonic speed at the exit of the discharge tube, therefore causally separating the upstream and downstream regions of the device.[20]

A cylindrical copper cathode surrounds the ceramic discharge tube of the PR, shown in Fig. 1 in orange. This electrode is connected to a RF power generator operating at 13.56 MHz which typically injects a forward input power up to 50 W after passing through a "L" impedance matching network ((2) and (3) in Fig. 4). The remainder of the device housing, made out of aluminium, is directly grounded and effectively acts as the anode for the capacitively coupled plasma (CCP) discharge. A dielectric ceramic housing separates the two electrodes (light grey in Fig. 1). At a given frequency, characteristic discharge dimension, pressure and gas ionization energy, a minimum voltage needs to be applied across the electrodes in order to breakdown the plasma by accelerating free electrons to sufficient kinetic energies that a cascade effect takes place. In PR, the typical dimension d is the discharge tube diameter. For argon and varying the pressure from 0.6 to 11 Torr, the PR breakdown voltage is plotted as a Paschen curve in Fig. 5 when the plenum electrode is grounded (Case 1). The minimum of the Paschen curve for Case 1 is ~200 V (peak voltage) obtained at 2.5 Torr. This voltage corresponds to an input power of less than 2 W. Owing to the large area asymmetry between the driven and grounded electrodes, the ceramic material under the driven electrode will locally charge negatively down to a so-called self-bias potential close to the applied peak RF voltage and will act as a blocking capacitor.[21] This negative potential is self-estlabished in order for the plasma to avoid breakdown of the sheath at the grounded electrode during the positive half of the RF cycle, as the plasma potential follows the applied RF potential oscillation. A beneficial side effect of the self-bias is the so-called γ mode. Under the driven electrode, ions are radially accelerated towards the tube to high energies through the sheath self-bias potential drop.[22] There, they impact the ceramic wall and release secondary electrons which are heated up in the sheath and ionize more propellant. This mode was demonstrated to be crucial in the working of the Pocket Rocket plasma discharge as it significantly increases the plasma density and hence the heating of the neutral propellant through charge-exchange ions-neutrals collisions.[21,22] Another important heating mechanism was shown to be the conduction heat transfer from the ceramic tube heated up from ion collisions, back to the neutral atoms.[23] Overall, these heating processes increase the thrust by up to 27% compared to cold gas operation, in some PR configurations.[17,24] The standard Pocket Rocket was a first experimental prototype while the Tiny Pocket Rocket is a miniaturization of the design made to accommodate the thruster on the DC-RF power inverter printed circuit board.[16]

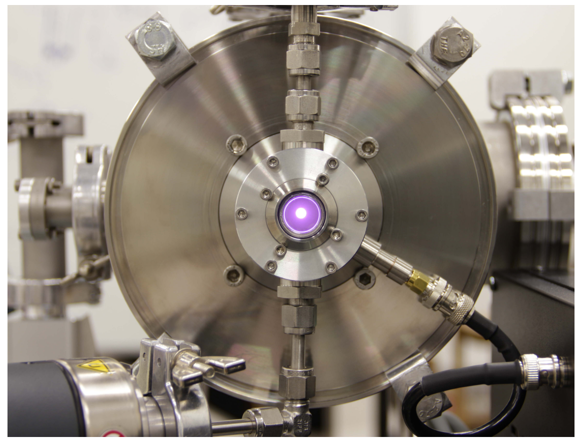

Figure 2. Close-up of the ePR in operation. The window can be replaced with diagnostics such as Langmuir probes in the present work.

B. The electron Pocket Rocket Neutraliser ePR

ePR is a prototype neutraliser based on the design of the Tiny Pocket Rocket but has a scale similar to the standard Pocket Rocket. The main difference being that the copper electrode dielectric and the discharge ceramic tube are jointly made in a single block of machinable ceramic. As the PR can provide plasma densities in excess of $10^{18}\,\mathrm{m}^{-3}$ for a few tens of Watts, after reaching operational equilibrium in the μs scale, it is believed to be a good candidate as an alternative to typical ion thruster hollow cathodes. Considering the aforementioned plasma density on axis of the discharge tube exit with an electron temperature of $\mathrm{T_e} = 2\,\mathrm{eV}$, as measured in previous studies,[15] a theoretical upper limit for the electron current can be given.
Assuming that no axial potential gradients exist to influence the plasma species dynamic, electrons and ions will wander through the exit of the discharge tube at their thermal random fluxes:

$$\Gamma_{\mathrm{e,th}} = \frac{1}{4}\sqrt{\frac{8T_{\mathrm{e}}}{\pi m_{\mathrm{e}}}};\quad \Gamma_{\mathrm{i,th}} = \frac{1}{4}\sqrt{\frac{8T_{\mathrm{e}}}{\pi M}}. \tag{1}$$

The discharge tube is a dielectric wall floating at Φ_{f} and for electrons in thermal equilibrium, the electron radial density profile follows the potential $\Phi(r)$ according to the Boltzmann relation:[25]

$$n_{\mathrm{e}}(r) = n_{\mathrm{s}} \exp\left(\frac{e\Phi(r)}{T_{\mathrm{e}}}\right), \tag{2}$$

where n_s is the plasma density of the presheath/sheath edge and r the radial coordinate. Approximating the total potential drop from the plasma bulk to a floating wall to $\sim -5.2T_\mathrm{e}$ for argon,[25] one can adjust the electron radial density profile to a Gaussian with a standard deviation giving the expected density at the wall and determine the equivalent Gaussian area $A_{\mathrm{G_e}}$ of the discharge tube.
Similarly, concidering ion flux continuity as the ions are radially crossing the presheath/sheath edge at the Bohm velocity, their density at the wall is given by:[25]

$$n_\mathrm{i} = n_\mathrm{s}\left(1 - \frac{2e\Phi_w}{Mu_B^2}\right)^{-\frac{1}{2}}. \tag{3}$$

In both cases, $n_\mathrm{s} = n\exp\left(\frac{-e\Phi_\mathrm{p}}{T_\mathrm{e}}\right)$ from the Boltzmann relation, with $\Phi_\mathrm{p} = \frac{T_\mathrm{e}}{2e}$ the minimum potential drop across the pre-sheath to satisfy Bohm's criterion and n the bulk plasma density. Again, adjusting the ion radial density profile to a Gaussian, one obtains the equivalent Gaussian area $A_{\mathrm{G_i}}$. Both electron and ion radial density profiles are represented in Fig. 3. Then, the electron and ion currents crossing the tube exit from random thermal flux are:

$$I_\mathrm{e} = eA_{\mathrm{G_e}}n\Gamma_{\mathrm{e,th}}; \quad I_\mathrm{i} = eA_{\mathrm{G_i}}n\Gamma_{\mathrm{i,th}}. \tag{4}$$

For values of $10^{18}\,\mathrm{m^{-3}}$ and 2 eV, this accounts for ~50.5 mA of electron current and ~0.6 mA of ion current. This demonstrates that if no potential gradient exists at the exit of the ePR, one can readily extract electrons thanks to their larger thermal flux compared to ions. Under this condition, an equal ion current needs to be lost somewhere else in the device in order to maintain the quasi-neutrality of the plasma. The condition of no potential gradient is unlikely to occur during the intended use of ePR. When operating on its own, i.e. when the ePR plasma plume expands into vacuum, a downstream plasma density decrease will have a corresponding plasma potential drop according to Boltzmann relation. Therefore low energy electrons will tend to be trapped into ePR and reduce the available $\mathrm{I_e}$. On the other hand, while neutralisers and ion beams coupling are not well understood, it is generally accepted that a potential gradient must exist between the neutraliser plasma and the ion beam in order for the electrons to overcome space-charge effects and neutralise the beam.[6,26] The existence of a so-called plasma bridge might lower this potential gradient by filling up the space between the neutraliser plasma and the ion beam with a quasi-neutral plasma.[27]

For the intended use of ePR, it would be ideal to lose all the discharge electrons at the tube exit and all ions inside the device. The only fluxes out of ePR should be electrons and neutrals that underwent a maximum number of ionization reactions in order to increase the gas utilisation fraction. The gas utilisation fraction is the ratio of extracted electron current to the used neutral particle equivalent current (1 sccm = 71.75 mA[1]). As species fluxes tend to be typically ambipolar in plasmas,[28] this implies modifying the nominal behaviour of the Pocket Rocket by establishing potential gradients and carefully sized loss areas. Following literature terminology, we name an "electron sheath" a sheath where all incident ions are reflected and all electrons can cross it, $\Delta\Phi_\mathrm{e} \gg T_\mathrm{i}/e$. Likewise, an "ion sheath" reflects all electrons $\Delta\Phi_\mathrm{i} \gg T_\mathrm{e}/e$. $\Delta\Phi_{e,i}$ are the potential drops across the electron and ion sheaths respectively, with respect to the bulk plasma potential.
A global nonambipolar flow is created when all plasma loss surfaces are either electron or ion sheaths.[29] In the standard PR configuration, the plenum is grounded and the locally developed sheath will be a standard sheath where some electrons will be lost. Most parts of the discharge tube will be floating at the floating potential Φ_w and also be an electron

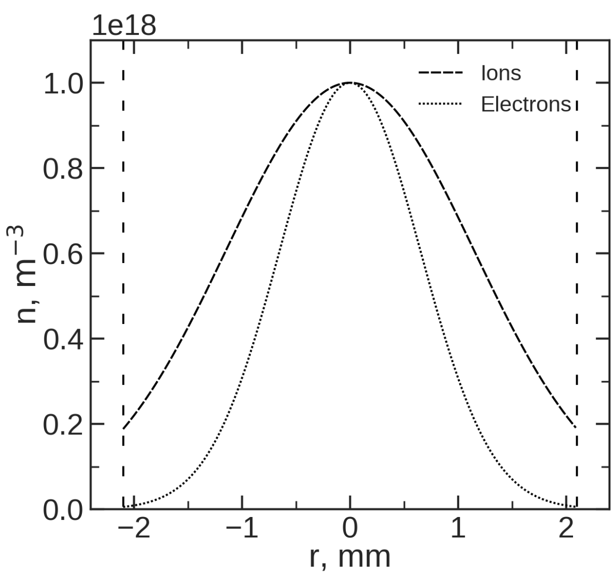

Figure 3. Gaussian approximations to electron and ion radial density profiles from the center bulk plasma density $\mathbf{n = 10^{18}\,m^{-3}}$ towards the floating discharge tube wall, for $\mathbf{T_e = 2\,eV}$. Vertical dashed lines represent the radial boundaries of the discharge tube.

well. The section of the tube under the driven electrode will be biased negatively at the maximum of the RF voltage and acts as a local ion sheath. The secondary electrons emitted from ion impacts in this region will have the same effect as if more ions have been lost locally. If we consider that the discharge tube exit experiences a steep potential gradient due to the presence of a surrounding ion beam, its cross section area A_{E} can be taken to behave as an electron sheath at a virtual positively biased electrode. Ignoring the discharge tube for simplicity, in ePR the ratio of the grounded plenum area A_{GP} to the discharge tube cross section is $A_{\mathrm{GP}}/A_{\mathrm{E}} \simeq 210$. According to the work in Ref.29, a monotonic electron sheath is created at the discharge tube exit (i.e. no ions can cross it but electrons can be lost to the grounded plenum) when the following condition is satisfied:

$$\frac{A_{\mathrm{GP}}}{A_{\mathrm{E}}} > \frac{1}{\mu} = \sqrt{\frac{e^1 M}{2\pi m_{\mathrm{e}}}} \simeq 178. \tag{5}$$

This is already an improvement compared to the the random thermal flux case described above, however electrons are still lost to the plenum wall. Following the work in Ref.29 and Ref.13, two possibilities exist to avoid electron collection in the plenum: reducing the surface of the grounded plenum to fall into the condition of a double sheath at the exit:

$$\frac{1}{\mu} > \frac{A_{\mathrm{GP}}}{A_{\mathrm{E}}} > \left(\frac{0.6}{\mu} - 1\right), \tag{6}$$

or applying a negative bias to the plenum walls such that $\Delta\Phi_{\mathrm{i}} \gg T_{\mathrm{e}}/e$ with area ratio:[13]

$$\frac{A_{\mathrm{PE}}}{A_{\mathrm{E}}} \simeq \sqrt{\frac{2M}{\pi m_{\mathrm{e}}}} \simeq 215, \tag{7}$$

where A_{PE} is the area of a biased plenum electrode (PE) and the right-hand side value is for argon.
A cylindrical hollow anode has been fitted into the plenum, as visible on the left-hand side of Fig. 1. To allow insertion of diagnostic instrumentation and as a first attempt, the PE used in this study does not cover the rear surface of the plenum and its area is only ~165 times that of the discharge tube cross section. Therefore, when the PE is grounded, it satisfies Eq.5 but does not satisfy Eq.7 when negatively biased. A complicating factor when establishing a nonambipolar flow in the ePR is that the potential of the discharge tube wall and the type of sheaths developed at this location cannot be controlled. However, the γ mode should beneficial for the operation of ePR as it increases the plasma density and therefore the gas utilisation fraction. With ions recombining on the discharge tube wall, they can be ionized several times before exiting the ePR, also increasing the gas utilisation.
To add more flexibility in controlling the potential gradient at the exit of the ePR, a so-called exit ring (ER) was placed right at this location. It extends the discharge tube by 6 mm without flow restriction and is made out of a stainless steel ring coated with a thin layer of boron nitride in order to avoid it collecting electrons while allowing a field to cross the floating dielectric. A 50 mm diameter disk is placed downstream of the ePR plume in order to collect electrons and is indicated as the chamber electrode (CE) in Fig. 1. Its distance from the tube exit can be varied. All three electrodes, the PE, ER and CE can be independently biased to positive or negative DC voltages or grounded. As a capacitively coupled plasma has strong plasma potential oscillation, the extracted electron current will be modulated by the driving frequency.

This study presents the first attempts at characterizing the electron production potential of the electron Pocket Rocket neutraliser. The overall goal is to maximize the usable electron current while minimizing the used RF and DC powers, the mass-flow rate and the voltage bias on electrodes.

III. Experimental Set-Up

A. Vacuum System

The experimental set up is shown in Fig. 4. The ePR is mounted on one of the faces of a 5.5 L cylindrical vacuum chamber (300 mm long 76.5 mm diameter) with ISO-K and ISO-KF interfaces ((1) in Fig. 4). Vacuum is primarily established with a roughing pump of 24 m^3/h pumping capacity and increased with a 250 L/s turbo pump if needed. As ePR operates in choked flow, the chamber background pressure has no influence on the gas flow and little influence on the plasma discharge as long as the pressure in the plenum is greater than twice the chamber pressure. The ePR is operated between 0.5 and 10 Torr of argon pressure

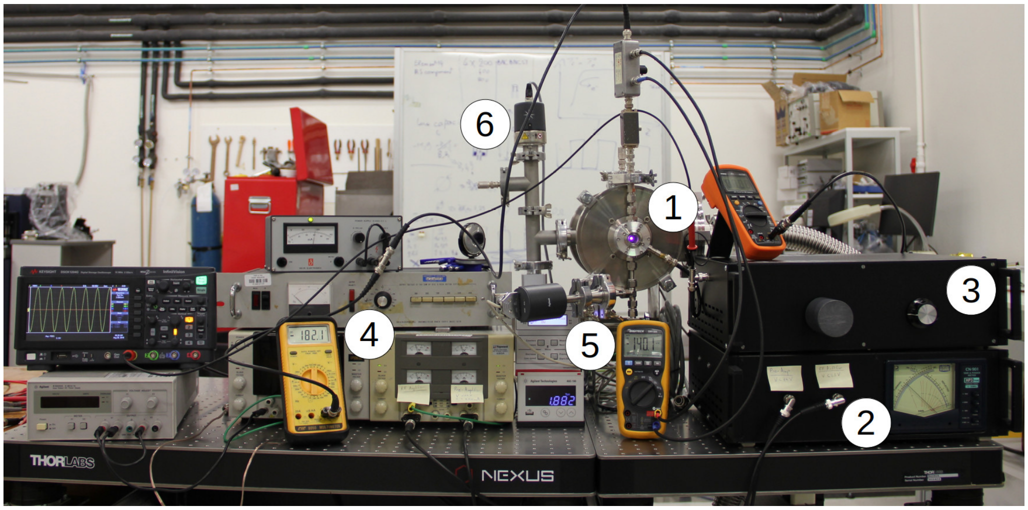

Figure 4. The ePR experimental apparatus. The electron source is mounted on a vacuum chamber (1) and powered with a custom made 50 W RF power amplifier (2). The input impedance of the ePR is matched to the 50 Ω output impedance of the amplifier by an L variable matching network (3). The experiment is fully powered by DC power supplies, both for plasma production and species extraction (4). The plenum pressure P_s is measured with a 0.2% accuracy capacitance diaphragm pressure gauge (5) while the vacuum level in the chamber is monitored with a full-range gauge (6).

in this study, which means the turbo pump was not needed as the primary pump achieves a sufficient base pressure of 10^{-4} Torr compared to 10^{-7} Torr with the turbo pump. A full-range Pirani / cold-cathode gauge tracks the vacuum level in the chamber ((6) in Fig. 4). The plenum pressure is measured with a 0.2% accuracy 100 Torr capacitance diaphragm pressure gauge ((5) in Fig. 4). The high capacity of the primary pump allows fast pump down times which accelerates operations after making modifications to the ePR or to the chamber.

B. Gas Feed

Argon is fed into the plenum of ePR through a $10 - 200$ sccm manual flow controller, separated from the chamber by a on-off ball valve. Owing to the low accuracy of the flow meter, the argon usage is instead evaluated from a reading of the plenum pressure. 100 sccm argon or 2.97 mg/s roughly corresponds to a plenum pressure of $P_s = 1.3$ Torr.

C. Diagnostics

For this study, a set of two single stainless steel planar Langmuir probes were used to determine the plasma parameters in the plenum, in the discharge tube and in the expanding plasma plume. The plenum Langmuir probe has a 2 mm diameter tip located at $z = -24$ mm and is axially centred with the discharge tube. The two degrees of freedom (translation/rotation) 1 mm diameter planar chamber Langmuir probe (LPC) is used to measure the plasma plume and can also be inserted into the discharge tube at the cost of disturbing the gas flow and the discharge. The probes are either allowed to float to measure the plasma floating potentials Φ_f or biased negatively and positively with respect to the plasma potential to measure the ion and electron saturation current. The latter measurements are made via the voltage drop across a measurement resistor placed in series with the probe. Measurements are made directly either via a digital oscilloscope or standard voltmeters. As this study is focussed on the RF averaged behaviour of the plasma, the RF components of the signals from the probe were filtered out by passive low-pass filters with a cut-off frequency at 1 MHz. Moreover, the dimensions of the plasma discharge makes it challenging to use RF compensated probes.
For the plasma density measurements reported in Section IV, the Langmuir probes were biased at -80 V in order to ensure to collect only ions. An electron temperature of 2 eV was assumed at these two locations, based on previous measurements reporting ~3 eV inside the discharge tube.[15] As the plasma expands from the heating region under the driven electrode, T_e is expected to decrease owing to heat and work exchange processes. The sheath expands with strong applied voltages on a wall.[25] Ref.30 gives a model of the sheath

expansion when biasing planar Langmuir probe for ion saturation current measurements. It is shown that the larger the area of the probe compared to the local Debye length, the less the sheath contribution to the effective ion collection area, asymptotically converging towards a factor 2 for probe radius more than 45 times the local Deybe length. Not taking the sheath area into account results in an overestimation of the plasma density. A sheath area to probe area ratio of 2 has been considered, as the limit to large Langmuir probes.[30] Therefore, the conversion of the ion saturation current to the plasma density was made using the formula:

$$n = \frac{I_{sat}}{e\kappa 2 A_{\rm p} u_{\rm B}}, \tag{8}$$

where $A_{\rm p}$ is the area of the probe, 2 is the correction factor for effective collection area and κ is the ratio of the plasma density at the sheath edge to the density in the plasma bulk, which was set to 0.55 as suggested in Ref.30. In addition to the probes, digital cameras are used to monitor relative changes in plasma luminosity and operation mode via two observation windows, one on the plenum axis as visible in Fig. 2 and Fig. 4 and one on a radial port of the vacuum chamber. A mirror in the vacuum chamber titled at 45° to the axial direction allows visualisation of the expanding plasma plume.

IV. Experimental Results

The experimental parameters for this study are: $P_{\rm rf} \in [1, 25]$ W, $P_{\rm s} \in [0.7, 2.0]$ Torr, bias voltage on the plenum electrode $\in [-320, 0]$ V, bias voltage on the chamber electrode $\in [0, 60]$ V and the exit ring is grounded. The RF power was kept below 25 W as the main foreseen application for the ePR would be for micro-ion thruster neutralisation. The lowest achievable value with the manual flow controller was 0.7 Torr and the onset of the γ mode required powers above 25 W at lower pressures.

A. Plasma Measurements

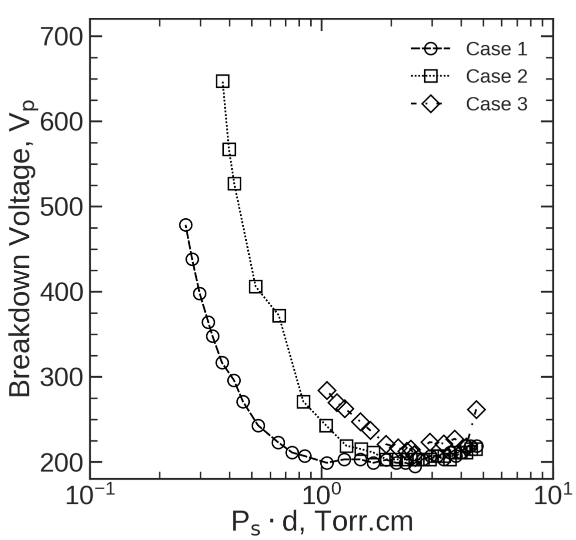

Figure 5. Paschen curves of ePR when the plenum electrode is grounded (Case 1), biased at −200 V (Case 2) and biased at −250 V (Case 3). d is the discharge tube diameter.

The first measurements performed were carried out for comparison with past studies on the Pocket Rocket, such as Ref.15.

Fig. 5 shows some ePR Paschen curves for three different situations, quantifying the influence of the plenum electrode bias on the plasma breakdown, measured with a HV probe at the exit of the matching network. As expected, when grounded, the inclusion of the plenum electrode and exit ring has not significantly modified the breakdown characteristic of the Pocket Rocket (Case 1 in Fig. 5) compared to previously reported results, since the electrodes simply replace the usual grounded section of the PR.[31]

When the plenum electrode is biased at −200 V and −250 V (Case 2 & 3 in Fig. 5), the minimum peak voltage for plasma breakdown is unchanged but occurs at a higher plenum pressure of ~5 Torr in both cases, compared to ~2.5 Torr when PE is grounded. This could be due to the electric field developed in the plenum and discharge tube repelling free electrons away from the discharge tube, requiring higher neutral pressures to reach the ionization collision mean-free path. This effect could be detrimental as optimisation of ePR will push for smaller mass-flow rates. The reason that the Case 3 curve starts at 1 $P_{\rm s}{\cdot}d$ is that a DC discharge takes place into the plenum at lower pressures, between the PE and grounded exposed parts of the plenum around the diagnostic aperture, even when no RF power is applied. The occurrence of this DC glow has a significant impact on the results of this study, as it will be discussed later.

The influence of the plenum electrode bias on the RF discharge was further characterized through the measurements of the floating plasma potential and plasma density at two key locations: slightly upstream of the entrance of the discharge tube ($z = -25$ mm) and at the exit of the discharge tube ($z = 0$ mm). These measurements were performed with the planar Langmuir probes and the results are reported in Fig. 6,7,8 and 9.

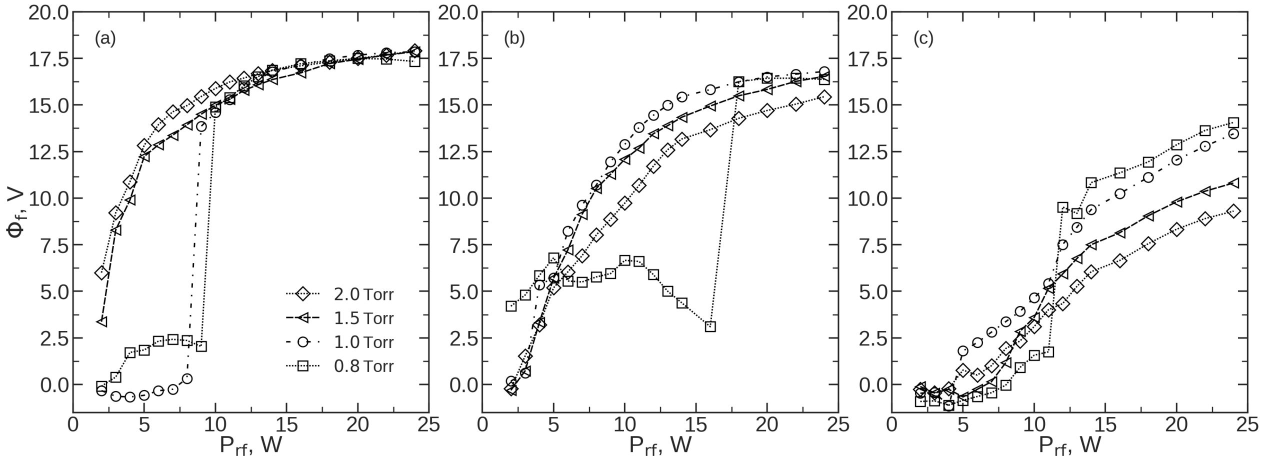

Figure 6. Plasma floating potential as measured with the chamber Langmuir probe at $z = 0$ mm, when the plenum electrode is grounded (a), biased at -200 V (b) and at -250 V (c).

Fig. 6 shows the floating plasma potential measured with the chamber Langmuir probe (LPC), right at the exit of the ePR (at the edge of the exit ring) for three different bias voltages applied to the plenum electrode. In this figure and in the subsequently, an abrupt mode transition is always observed for the cases $P_s = 0.8$ Torr (square markers). When $P_s = 1.0$ Torr (circle markers) and PE is grounded, the same transition is observed but is smoother for -200 V and -250 V on PE. This transition is attributed to the onset of the γ mode of the capacitively coupled discharge, which usually requires high neutral densities for small enough ionization mean-free path between the secondary electrons released from the ceramic wall and the neutral gas.[25] When in α mode (stochastic heating), the discharge glow is much fainter and the plasma stays confined into the plenum and discharge tube. When the γ mode is triggered, a bright plasma plume expends downstream into the vacuum chamber, the overall brightness into the discharge tube increases and switches from pink/purple to blue/purple, indicating the de-excitation of electrons from higher argon orbitals. This transition has been captured on camera and reported in Fig. 10 at $P_s = 1.25$ Torr.

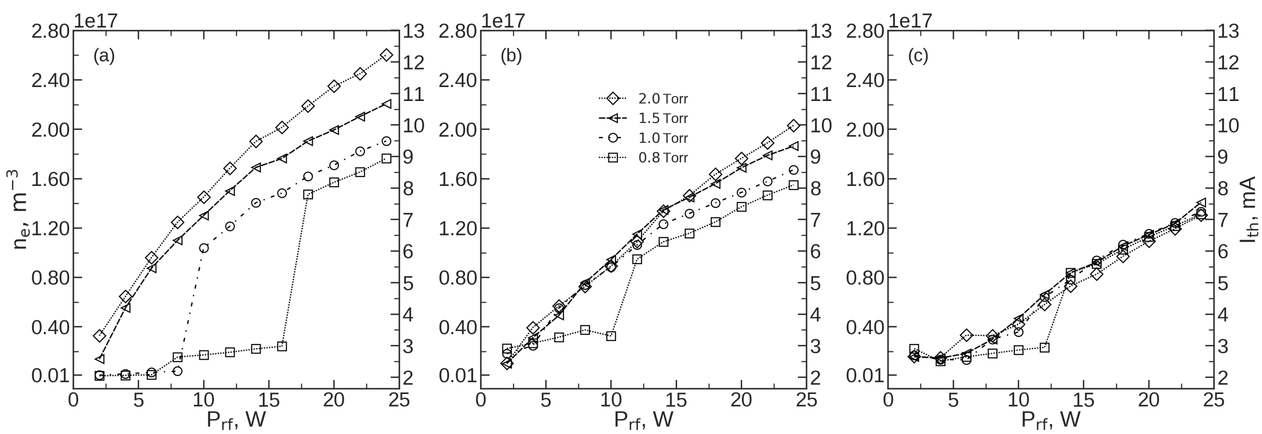

Figure 7. Plasma density as measured by the chamber Langmuir probe (LPC) located at $z = 0$ mm, when the plenum electrode is grounded (a), biased at -200 V (b) and at -250 V (c). Right y axis gives the corresponding thermal net current out of the discharge tube $I = I_e - I_i$ according to Eq.4.

This mode transition explains the much lower measured floating potentials at $P_s = 0.8$ Torr and $P_s = 1.0$ Torr in Fig. 6 as the LPC is probing much weaker densities when the plasma stays confined into ePR. The measured levels of Φ_f are coherent with previous numerical simulations results, which reported for example a RF cycle average plasma potential of 27 V at 5 W and 1.5 Torr under the driven RF electrode. Taking 2 eV, $\Phi_p = \Phi_f + 5.2T_e = 25.5$ V for similar parameters when PE is grounded, which is lower than the value under the electrode due to plasma diffusion. When the plenum electrode is biased, the floating potential levels at the exit of ePR are only slightly affected at −200 V while changes are more significant at −250 V (Fig. 6, (c)). There, discharges at lower pressures are less affected. Overall, the PE is unable to strongly affect the potential gradients in the discharge tube, as the latter represents an intermediate floating plasma boundary, clamping it to values close to the standard Pocket Rocket operation.

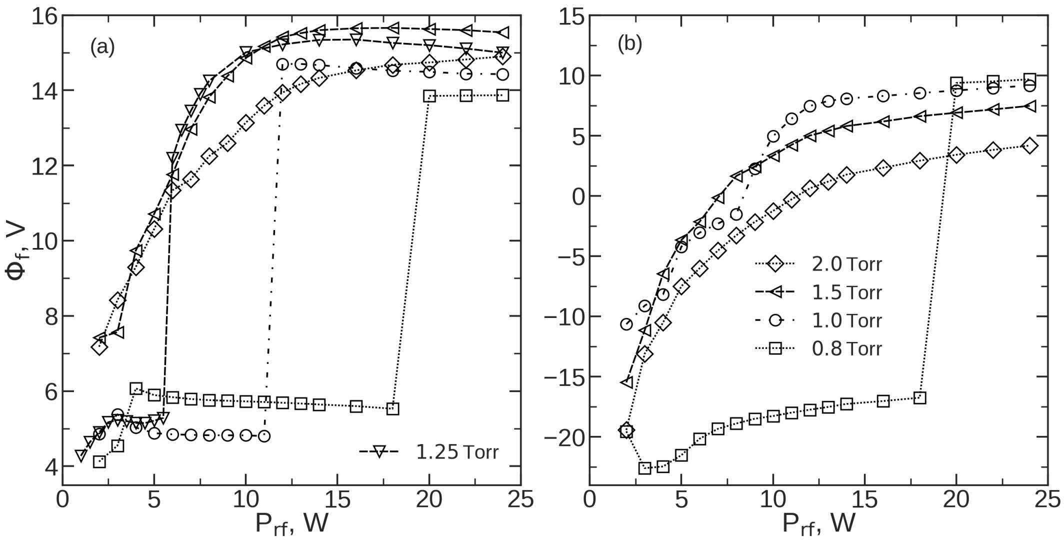

Figure 8. Plasma floating potential as measured with the plenum Langmuir probe at z = −25 mm, when the plenum electrode is grounded (a) and when it is biased at −200 V (b). Graph (a) includes an additional curve at $P_s = 1.25$ Torr.

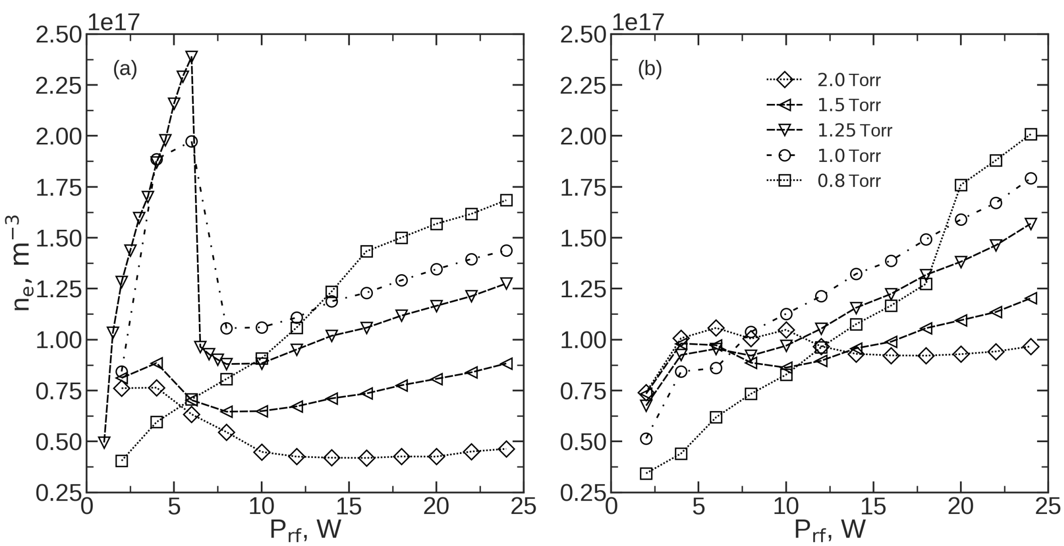

Figure 9. Plasma density measured by the plenum Langmuir probe located at z = −25 mm, when the plenum electrode is grounded (a) and when it is biased at −200 V (b). The high density confined plasma mode is clearly visible for $P_s = 1.0$ Torr and 1.25 Torr.

Fig. 7 gives the plasma densities corresponding to the same conditions as in Fig. 6. Matching the conclusions of the floating potential measurements, the curves for the grounded plenum electrode (a) show that the mode transition corresponds to a step increase in density in the plume of ePR for the cases 1.0 Torr and 0.8 Torr. The plasma density is otherwise $\propto \sqrt{P_{rf}}$ as characteristic to capacitively coupled discharges.[25]

A net decrease in plasma density when the plenum bias was applied was observed and visible in Fig. 7 (b) and (c). A possible explanation is that with the onset of the DC discharge came a net density increase in the plenum and the discharge tube plasma gets attracted upstream by the negative bias of the PE. More surprising is the decrease in the δn_e between different pressures at a given power visible in Fig. 7 (c) when the plenum is biased at -250 V. Now, the density has locally decreased by a factor 2 compared to the case when the PE is grounded and the plenum pressure has negligible influence for $P_{rf} > 15$ W. According to the axial plasma density profile reported in Ref. 15, the plasma density measured in the grounded case at 24 W and 2.0 Torr should corresponds to a peak density in the discharge tube close to $5 \cdot 10^{17}\,m^{-3}$
Fig. 8 and Fig. 9 report the same measurements as Fig. 6 and Fig. 7, 2 mm upstream of the discharge tube, in the plenum, when the PE is grounded (a) and biased at -200 V (b). Measurements at -250 V were not performed as the Langmuir probe was placed so close to the PE that arcing events were occurring at more negative bias. When the PE is grounded, the plasma floating potential behaves in a manner similar than at the discharge tube exit (Fig. 6 (a)). However, Fig. 9 (a) shows that the plasma density has the opposite behaviour than the downstream region of ePR: the plenum experiences significant density peaks at $P_s = 1.0$ Torr and 1.25 Torr while it stays relatively low at higher pressures and even experiences decreases for increasing RF power at the highest pressures. This opposite behaviour of the plasma density upstream and downstream of the discharge tube as a function of the set plenum argon pressure appear to be due to a mode of operation when the plasma is confined into the plenum and the discharge tube and does not significantly expends downstream.
This confined mode was observed to be at an optimum when the plenum pressure was set somewhere between 1.0 Torr and 1.3 Torr and for RF powers below 6 W. At these conditions, no visually appreciable plasma was getting further down than $z = 0$ mm, i.e. than the downstream edge of the exit ring. Fig. 10 attempts to share this observation. The conditions are $P_{rf} \in [2, 5.75]$ W and $P_s = 1.25$ Torr, matching the peak displayed in Fig. 9 (a). As the RF power in carefully increased, the plasma becomes appreciably brighter and bluer and take the shape of a water drop whose edge does not exceed the exit ring. Between 5.5 W and 5.75 W, the plasma suddenly forms a bright plume expanding downstream. As the plasma floating potential under these conditions has relatively low values, even negatives downstream to the extraction ring (circle markers in Fig. 6 (a)), it could be that the grounded exit ring applies a potential barrier that the plasma can only break when the γ mode and its correspondingly higher floating potentials takes place. This would mean than under α mode operation, the plasma floating potentials are negative in the discharge tube and an electron sheath could be established at the exit of ePR.

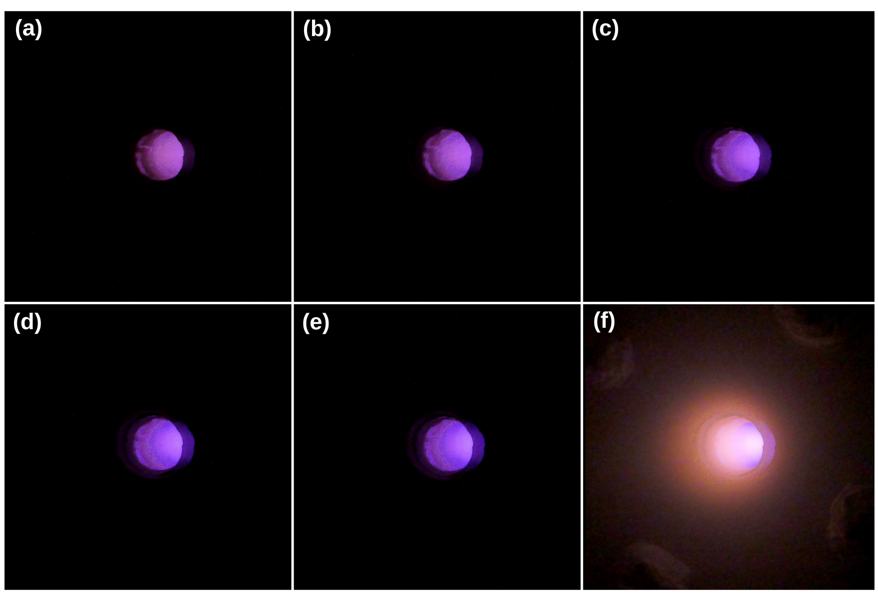

Figure 10. Transition between the high density confined plasma mode and the diffuse plasma mode. The RF power is set at 2 W (a) to 3 W (b), 4 W (c), 5.0 W (d), 5.5 W (e) and 5.75 W (f). The plenum pressure is fixed at 1.25 Torr and the plenum electrode is grounded.

When a bias is applied on the plenum electrode, the confined mode is not observed any more although

Fig. 9 (b) shows that the density still peaks around 5 W at the concerned pressures. Of potential interest for the ePR operation, the plasma densities in the plenum are greater for lower plenum pressures, both when the PE is grounded and biased. This would allow a larger ion current to be collected in the plenum and incidently a larger electron current extractable downstream for neutralisation.

B. Ions and Electrons Extraction

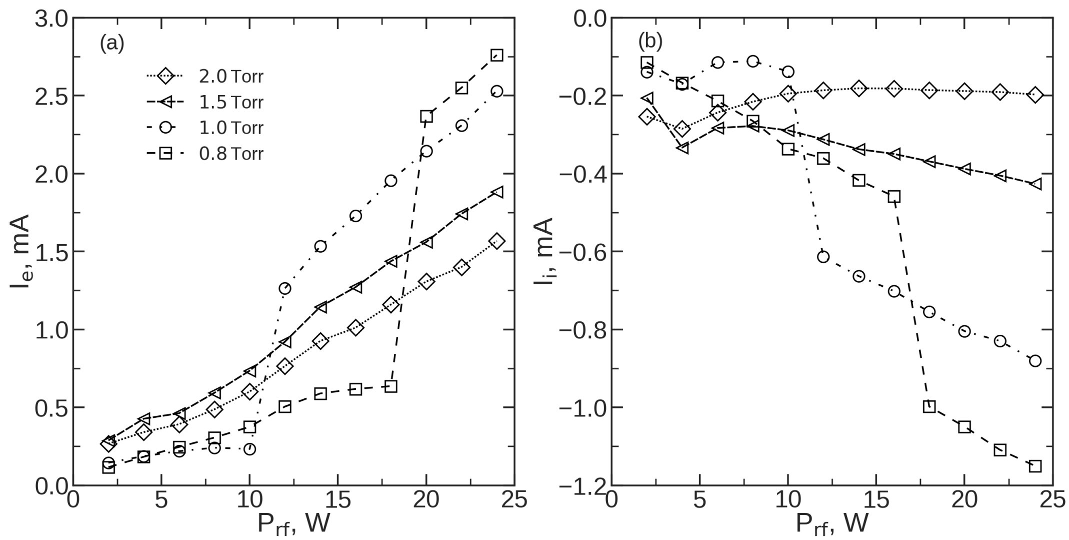

Figure 11. (a) Electron current as collected by the Chamber Electrode (CE) biased at 30 V at z = 15 mm as a function of the RF power and for various plenum argon pressures. (b) Ion current as collected by the grounded plenum electrode under similar conditions.

The first indications of the electron production capabilities of the Pocket Rocket resulted from the high plasma density measured in its plume, slightly over $10^{18}\,\mathrm{m}^{-3}$ at $P_{rf} = 33\,\mathrm{W}$.[18] In order to evaluate the current which can be extracted from the ePR in this simple configuration, i.e. while the plenum electrode is left grounded, the Chamber Electrode (CE), a 50 mm diameter disk, was placed 15 mm downstream of the exit ring and biased at +30 V. The choice of the bias voltage value will be detailed below. As visible in Fig. 11 (a), up to 2.76 mA is collected by the CE for $P_{rf} = 24\,\mathrm{W}$ and $P_s = 0.8\,\mathrm{Torr}$. The electron current is inversely proportional to the operating pressure. This is counter-intuitive as the plasma density measured in the ion saturation regime by the LPC at the same location is proportional to P_s, as seen in Fig. 7 (a). A potential explanation is the need for a balancing ion current to be lost somewhere else in the system.

The net current being collected on the grounded PE while electrons are extracted by the CE is shown in Fig. 11 (b). In the plenum, lower argon plenum pressures correspond to higher plasma densities as reported in Fig. 9, while the floating potential stays constant is in the order of 15 V. Hence, it is natural to observe a net larger ion current (counted as negative) being collected at low P_s in Fig. 11 (b). In consequence, the condition $I_e = I_i$ is better fulfilled at lower operating pressures, which could explain the higher extracted electron current.

For the plasma densities measured by the LPC at the exit of ePR and for $T_e = 2\,\mathrm{eV}$ and according to the development of Eq.4, the expected net thermal current $I_e + I_i$ (I_i still counted as negative) is reported on the right vertical axes of Fig. 7. Comparing the values of Fig. 11 (a) to Fig. 7 (a), one can see that we are below the expected available electron current. The suspected cause is that the plasma density in the plenum volume is too low in the configuration for a sufficient amount of ions to be collected there. Previous numerical simulations showed that the plasma density in the plenum is indeed peaked on axis with the discharge tube entrance but decreases exponentially both axially and radially.[17,21] It was therefore decided to explore the influence of a negative bias applied on the plenum electrode.

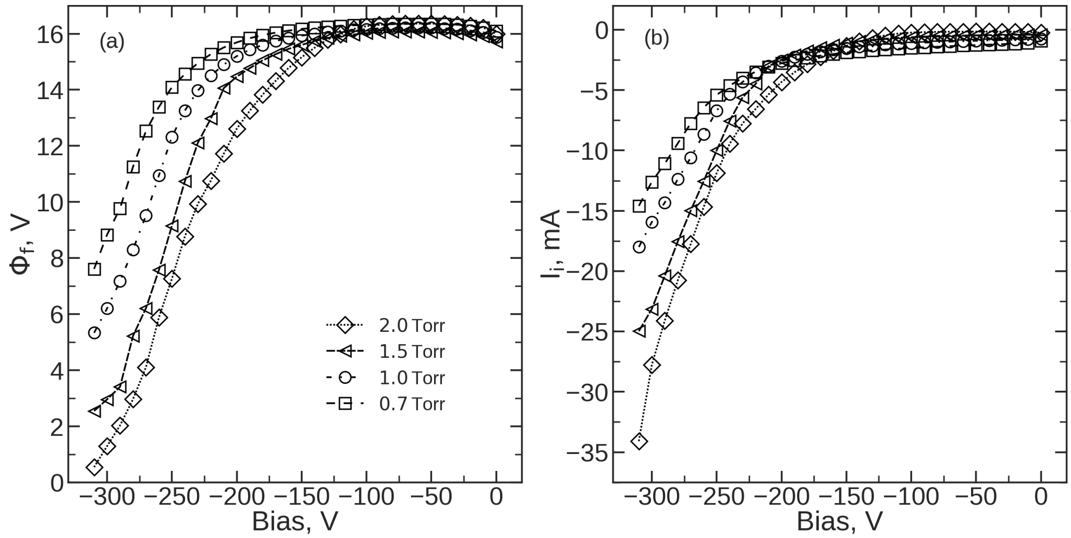

Figure 12. Plasma floating potential at $z = 0$ mm (a) and ion current collected on the plenum electrode (b) for increasing plenum electrode bias voltage, for various plenum pressures and $P_{rf} = 15$ W.

Fig. 12 shows the plasma floating potential at the exit of the discharge tube as measured with the LPC (a) and the amount of ion current I_i collected on the plenum electrode when its bias is varied from 0 V to −310 V. Above ~ -200 V, both the floating potential and the ion current stay mostly constant. The small increase in I_i is probably due to rejection of the Maxwellian tail high energy electrons by the sheath developed on the plenum electrode and therefore to the onset of a pure ion sheath. However, as the plasma density in the plenum is low, increasing the bias voltage does not increase the ion current significantly. But when there is no more, there is more. As the DC discharge is initiated into the plenum for lower bias voltages, a net increase of I_i is observed as the plasma density of the DC discharge increases with the applied bias. Interestingly, the floating potential measured at the exit ring ($z = 0$ mm) follows roughly the same dependency, possibly due to a drain of the ions even down into the discharge tube (Fig. 12 (a)). For the lowest bias of −310 V and for $P_s = 2.0$ Torr, the floating potential is about 0.5 V and is likely to decrease axially towards the plenum. Under such conditions, it is possible that an electron sheath is setting along the discharge tube while an ion sheath is definitely set on the plenum electrode ($\Delta\Phi_i \gg T_e/e$).

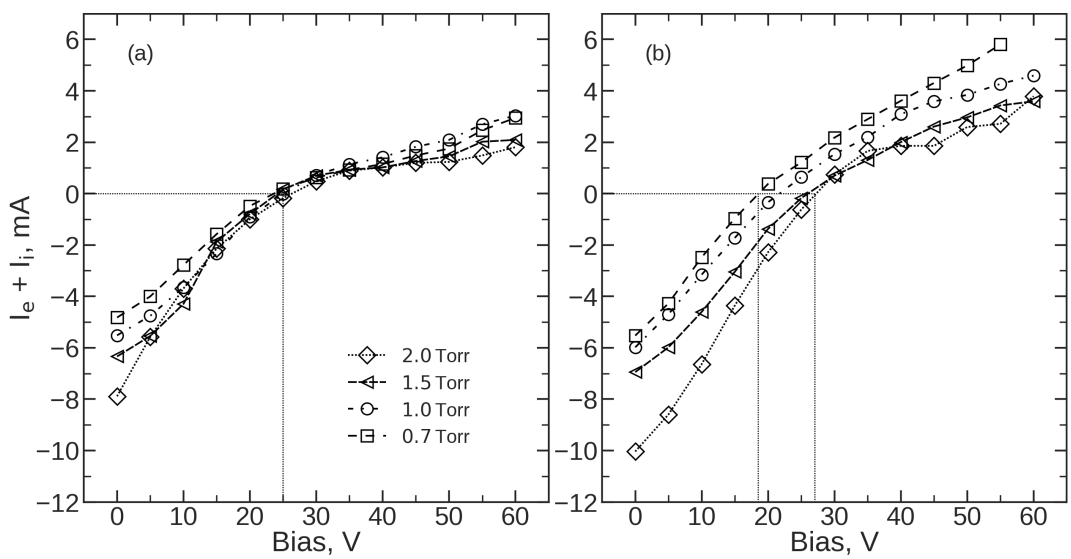

Figure 13. Sum of the electron current collected by the chamber electrode and the ion current collected by the plenum probe as the chamber electrode bias is increased, for $P_{rf} = 15$ W (a) and $P_{rf} = 25$ W (b) and various plenum pressures. The plenum electrode bias is fixed at −250 V. Dotted lines indicate the points of current balance.

With ion currents in excess of the expected downstream random electron flux, the chamber electrode was either grounded or biased up to +60 V in order to evaluate the available electron currents. Fig. 13 reports the sum of the electron current (positive sign) and of the ion current (negative sign) collected by the chamber electrode and the plenum electrode respectively, as the bias of the CE is increased and while the PE is biased at −250 V. It can be seen that when the CE has biases lower than ~20 V, the ion current dominates the balance. As the bias on CE increases, the electron current steadily takes over, although it has to be noted that the ion current on the plenum electrode was also increasing with the CE bias, but at a lower rate. It is very interesting to observe a plateau happening when the two currents get close to each other, particularly visible for $P_{rf} = 15$ W (Fig. 13 (a)). Current balance occurs for a bias of 25 V when $P_{rf} = 15$ W with little variation between the different pressures. When the RF power is increased to 25 W, a spread occurs as lower pressures require lower biases (18.5 V) and higher pressures slightly higher biases (27 V). At these points, it is tempting to think of a nonambipolar flow taking place into the ePR, but more investigations are necessary to understand the role and influence of the discharge tube. When the CE bias potential is higher than 30 V, the electron current extracted downstream becomes larger than the ion current extracted upstream, possibly due to the bias of the chamber electrode exceeding the local plasma potential and draining electron currents above the thermal flux by establishing a potential well for the electrons to get accelerated into. Therefore, when the plenum electrode is biased so negatively as to trigger a DC discharge in the plenum, the local increase of plasma density enables much larger ion currents to get collected on the PE and coincidently higher electron currents to get extracted out of the ePR by an electrode biased at roughly the local plasma potential.

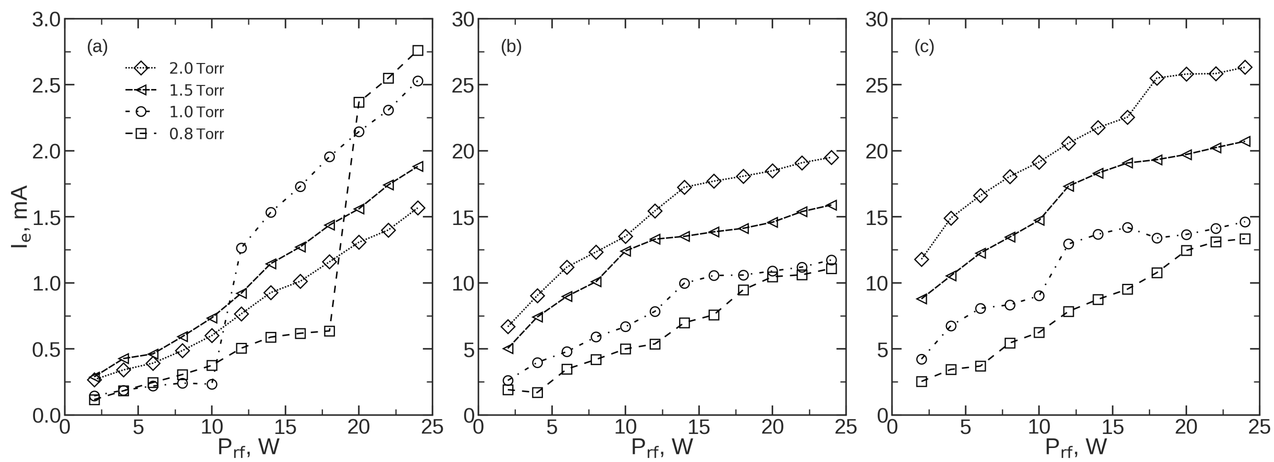

Figure 14. Electron current as a function of the RF power for the cases when the ion plenum electrode is grounded (a), biased at −250 V (b) and −270 V (c). The bias on the chamber electrode is set at 30 V to guarantee current balance in all cases.

Finally, Fig. 14 gives an overview of the two cases discussed above: extracted electron current when the plenum electrode is grounded (a) and when it is biased negatively at −250 V (b) and −270 V (c). According to the development in Section II,B, when the PE is grounded (Fig. 14 (a)), the condition for a monotonic electron sheath could be satisfied at the exit of ePR (again, overlooking the role of the discharge tube boundary). Thus, all ions and some electrons should be lost to the plenum walls and the entire thermal electron flux should be extracted at the exit of ePR. This does not occur as the measured electron current levels are several times lower than the estimate of the thermal electron current according to the density measurements (right y axis of Fig. 9 (a)). It is certain that the role of the discharge tube wall can not be neglected when characterizing the current balance in ePR with a grounded plenum.

The same is true when the PE is biased negatively and as electron currents greater than the thermal fluxes are measured on the CE (Fig. 14 (b), (c)). In this regime, Eq.7 should be satisfied in order for a total nonambipolar flux to take place. However, the area of the plenum electrode employed in this preliminary study is too small to fulfil the condition in Eq.7 condition. Here again, the influence of the discharge tube wall would explains this (beneficial) discrepancy with the analytical model as the self-bias charging of the wall and the secondary electrons emission undeniably contribute to the particle balance. In a future work, resolving the RF oscillation of the plasma potentials could also be essential for a better characterisation of the species fluxes as all the quantities reported in this work are averaged over the RF cycle.

V. Conclusion

The first empirical attempts at evaluating the capacity of the Pocket Rocket to be used as an ion thruster neutraliser have shown that two modes of operation exist in the current configuration. When the plenum electrode charged to be the main ion loss surface is grounded, electron currents well below values expected from simple random thermal flux estimations are measured on a downstream located chamber electrode. In this mode, the ion current collected in the plenum is always below the electron current collected by the CE. Therefore, losses on other surfaces must be occurring to maintain plasma quasi-neutrality, probably on the discharge tube wall. The low performance is due to plasma densities being too low in the plenum, since the extractable electron current is dependant on the collected ion current. When the plenum electrode is biased sufficiently negative such as to trigger a DC discharge in the plenum (< -200 V), the plasma density is visually locally much higher. In this mode, the ion current collected on the plenum electrode increases monotonically with the bias, to values greater than -20 A. Ion-electron current balance is achieved when the chamber electrode is biased roughly above 30 V, which corresponds to the local plasma potential. An electron current up to 41 mA was measured for ~50 W, 2.0 Torr and with the plenum electrode biased at -320 V. Future work will focus on increasing the electron current while decreasing or removing the plenum electrode bias. Negatively biased electrodes would significantly affect the lifetime of the ePR and should be avoided. Trials with different discharge tube materials and geometries, especially with smaller discharge tube exit cross-section areas are planned. Attention should be focused on reducing the plasma loss areas and maximizing the plasma density at the exit of the ePR. This simple modification should allow the maintainance of the beneficial γ mode at much lower argon mass-flow rates. The experimental apparatus will be continuously improved with the use of a high accuracy digital flow controller and the design and use of automated Langmuir probe measurement system for complete and fast plasma parameters characterization. Numerical simulations will be carried using a computational fluid dynamic model based on previous works on Pocket Rocket and will greatly ease the optimization of the ePR. Development of low power high efficiency power amplifiers and matching circuits are continuing at ANU and Stanford University,[16] while propellant subsystem prototyping is carried out at Cal Poly[32] and at the University of Auckland (Fig.15). These developments will allow ePR to be a operated as a stand-alone subsystem.

Figure 15. Prototype propellant subsystem with commercial off-the-shelf components: proportional valve, pressure regulator, pressure sensor and argon canisters.

Acknowledgments

This work is supported by the New Zealand Space Agency (NZSA), Ministry of Business Innovation and Employment (MBIE). We would like to thank Loevan Michel for his work on the propellant subsystem development.

References

[1]D. M. Goebel and I. Katz, *Fundamentals of Electric Propulsion: Ion and Hall Thrusters*. JPL Space Science and Technology Series, 2008.

[2]T. R. Sarver-Verhey, "Scenario for hollow cathode end-of-life," *NASA Contractor Report*, 2000.

[3]D. Goebel, "Extending hollow cathode life for electric propulsion for long-term missions," in *Space 2004 Conference and Exhibit*, (San Diego, U.S.A.), p. 5911, 2004.

[4]A. Sengupta, "Destructive physical analysis of hollow cathodes from the Deep Space 1 flight spare ion engine 30,000 hr

life test," 2005.

[5]I. M. Ahmed Rudwan, N. Wallace, M. Coletti, and S. Gabriel, "Emitter depletion measurement and modeling in the T5 & T6 kaufman-type ion thrusters," 2007.

[6]J. E. Foster, G. J. Williams, and M. J. Patterson, "Characterization of an ion thruster neutralizer," *Journal of Propulsion and Power*, vol. 23, no. 4, pp. 828–835, 2007.

[7]G. Becatti, D. M. Goebel, J. E. Polk, and P. Guerrero, "Life evaluation of a lanthanum hexaboride hollow cathode for high-power hall thruster," *Journal of Propulsion and Power*, vol. 34, no. 4, pp. 893–900, 2017.

[8]R. Lewis, J. P. Luna, and F. Guarducci, "Qualification of the t6 thruster for bepicolombo," in *34th International Electric Propulsion Conference and 6th Nanosatellite Symposium, Hyogo-Kobe, Japan*, 2015.

[9]Y. Tsuda, M. Yoshikawa, T. Saiki, S. Nakazawa, and S.-i. Watanabe, "Hayabusa2–sample return and kinetic impact mission to near-earth asteroid ryugu," *Acta Astronautica*, vol. 156, pp. 387–393, 2019.

[10]D. Lev, R. M. Myers, K. M. Lemmer, J. Kolbeck, H. Koizumi, and K. Polzin, "The technological and commercial expansion of electric propulsion," *Acta Astronautica*, 2019.

[11]D. A. Herman, T. A. Tofil, W. Santiago, H. Kamhawi, J. E. Polk, J. S. Snyder, R. R. Hofer, F. Q. Picha, J. Jackson, and M. Allen, "Overview of the Development and Mission Application of the Advanced Electric Propulsion System (AEPS)," *NASA Technical Report*, 2018.

[12]T. Ito, N. Gascon, W. S. Crawford, and M. A. Cappelli, "Experimental characterization of a micro-hall thruster," *Journal of Propulsion and Power*, vol. 23, no. 5, pp. 1068–1074, 2007.

[13]B. Longmier, S. Baalrud, and N. Hershkowitz, "Nonambipolar electron source," *Review of Scientific Instruments*, vol. 77, no. 11, 2006.

[14]M. Tsay, J. Frongillo, J. Zwahlen, and L. Paritsky, "Maturation of iodine fueled bit-3 rf ion thruster and rf neutralizer," in *52nd AIAA/SAE/ASEE Joint Propulsion Conference*, p. 4544, 2016.

[15]C. Charles and R. Boswell, "Measurement and modelling of a radiofrequency micro-thruster," *Plasma Sources Science and Technology*, vol. 21, no. 2, p. 022002, 2012.

[16]W. Liang, C. Charles, L. Raymond, A. Stuchbery, K. Surakitbovorn, L. Gu, R. W. Boswell, and J. M. Rivas Davila, "An integrated RF power delivery and plasma micro-thruster system for nano-satellites," *Frontiers in Physics*, vol. 6, p. 115, 2018.

[17]T. S. Ho, C. Charles, and R. Boswell, "Performance modelling of plasma microthruster nozzles in vacuum," *Journal of Applied Physics*, vol. 123, no. 17, p. 173301, 2018.

[18]S. Dixon *et al.*, *Experimental study of expanding hollow cathode discharges.* PhD thesis, The Australian National University, 2015.

[19]R. Boswell, C. Charles, P. Alexander, J. Dedrick, and K. Takahashi, "Plasma expansion from a radio frequency microdischarge," *IEEE Transactions on Plasma Science*, vol. 39, no. 11, pp. 2512–2513, 2011.

[20]T. S. Ho, C. Charles, and R. W. Boswell, "A comprehensive cold gas performance study of the pocket rocket radiofrequency electrothermal microthruster," *Frontiers in Physics*, vol. 4, p. 55, 2017.

[21]T. S. Ho, C. Charles, and R. Boswell, "Redefinition of the self-bias voltage in a dielectrically shielded thin sheath rf discharge," *Journal of Applied Physics*, vol. 123, no. 19, p. 193301, 2018.

[22]T. S. Ho, C. Charles, and R. Boswell, "Neutral gas heating and ion transport in a constricted plasma flow," *Physics of Plasmas*, vol. 24, no. 8, p. 084501, 2017.

[23]A. Greig, C. Charles, and R. W. Boswell, "Spatiotemporal study of gas heating mechanisms in a radio-frequency electrothermal plasma micro-thruster," *Frontiers in Physics*, vol. 3, p. 84, 2015.

[24]C. Charles, R. W. Boswell, A. Bish, V. Khayms, and E. F. Scholz, "Direct measurement of axial momentum imparted by an electrothermal radiofrequency plasma micro-thruster," *Frontiers in Physics*, vol. 4, p. 19, 2016.

[25]M. A. Lieberman and A. J. Lichtenberg, *Principles of plasma discharges and materials processing.* John Wiley & Sons, 2005.

[26]H. Usui, A. Hashimoto, and Y. Miyake, "Electron behavior in ion beam neutralization in electric propulsion: full particle-in-cell simulation," in *Journal of Physics: Conference Series*, vol. 454, p. 012017, IOP Publishing, 2013.

[27]V. K. Rawlin and E. V. Pawlik, "A mercury plasma-bridge neutralizer.," *Journal of Spacecraft and Rockets*, vol. 5, no. 7, pp. 814–820, 1968.

[28]F. Chen, "High density plasma sources," *Materials Science and Process Technology Series, Noyes Publications*, pp. 1–75, 1995.

[29]S. Baalrud, N. Hershkowitz, and B. Longmier, "Global nonambipolar flow: Plasma confinement where all electrons are lost to one boundary and all positive ions to another boundary," *Physics of plasmas*, vol. 14, no. 4, p. 042109, 2007.

[30]T. Sheridan, "How big is a small Langmuir probe?," *Physics of Plasmas*, vol. 7, no. 7, pp. 3084–3088, 2000.

[31]C. Charles, R. Boswell, and K. Takahashi, "Investigation of radiofrequency plasma sources for space travel," *Plasma Physics and Controlled Fusion*, vol. 54, no. 12, p. 124021, 2012.

[32]P. Van Ness, G. Ramirez Jr, S. Gnagy, S. Diamantopoulous, and A. Greig, "Pressurized 1U CubeSat Propulsion Unit," in *33rd Annual AIAA/USU Conference on Small Satellites*, (Logan, U.S.A.), pp. 1–8, 2019.